PHYSICAL REVIEW A **84**, 053202 (2011)

Electron spectra of xenon clusters irradiated with a laser-driven plasma soft-x-ray laser pulse

S. Namba,[1] N. Hasegawa,[2] M. Kishimoto,[2] M. Nishikino,[2] K. Takiyama,[1] and T. Kawachi[2]
[1]*Graduate School of Engineering, Hiroshima University, 1-4-1 Kagamiyama, Higashi-Hiroshima, Hiroshima 739-8527, Japan*
[2]*Quantum Beam Science Directorate, Japan Atomic Energy Agency, 8-1-7 Umemidai, Kizugawa, Kyoto 619-0215, Japan*
(Received 15 September 2011; published 14 November 2011)

Xenon clusters were irradiated with plasma soft-x-ray laser pulses (having a wavelength of 13.9 nm, time duration of 7 ps, and intensities of up to 10 GW/cm^2). The laser photon energy was high enough to photoionize 4*d* core electrons. The cross section is large due to a giant resonance. The interaction was investigated by measuring the electron energy spectra. The photoelectron spectra for small clusters indicate that the spectral width due to the 4*d* hole significantly broadens with increasing cluster size. For larger clusters, the electron energy spectra evolve into a Maxwell-Boltzmann distribution, as a strongly coupled cluster nanoplasma is generated.

DOI: 10.1103/PhysRevA.84.053202 PACS number(s): 36.40.Gk, 32.80.Hd, 52.50.Jm

I. INTRODUCTION

Since the invention of chirped-pulse amplification for ultrashort laser systems [1], much effort has been devoted to understanding the interaction of high-intensity laser pulses with matter [2]. In particular, a rare-gas cluster that is classified as an intermediate state between isolated atoms and bulk solid-state matter has attracted considerable attention as a target [3,4], because it shows unique properties such as efficient absorption of laser photons leading to Coulomb explosions of a cluster [5], generation of bright x-ray radiation [6], and formation of energetic ions up to MeV [7].

Experiments to elucidate the interaction of short-wavelength laser pulses with clusters have previously been carried out using a vacuum-ultraviolet free-electron laser (VUV-FEL) at a wavelength of 98 nm [8]. The results indicated that (i) each atom within a large cluster absorbs on the order of 30 photons, (ii) the kinetic energy of the Xe^{7+} ions is as high as 2 keV, and (iii) the clusters disintegrate into isolated atomic fragments after a Coulomb explosion. Various experimental [9,10] and theoretical [11–16] studies have been conducted to provide a deeper understanding of photoabsorption within clusters and the subsequent explosion dynamics in the short-wavelength regime.

Recent progress in FEL technology has enabled researchers to make use of intense, ultrashort x-ray laser pulses [17,18]. A free Xe atom was exposed to a FEL pulse having a wavelength of 13.3 nm (photon energy of 93 eV) and an intensity of 10 PW/cm^2 [19], where pumping of Xe 4*d* inner electrons becomes possible (at an ionization potential of 67.55 eV for $4d_{5/2}$ and 69.54 eV for $4d_{3/2}$). Surprisingly, a mass peak attributed to the Xe^{21+} ion was observed, implying that conventional perturbative and nonperturbative descriptions fail to account for photoabsorption of extremely intense x-ray laser pulses. On the other hand, Bostedt *et al*. examined the interaction of a 32.8 nm FEL pulse with Ar clusters [20]. They found that, with increasing laser intensity, the photoelectron spectra varied from the results obtained for a free atom due to the multistep electron emission from the clusters; a nanoplasma formed at a threshold laser intensity of 50 TW/cm^2. Moreover, the interaction of the FEL pulses in the 13 nm wavelength region with large Xe clusters was investigated [21–23]. A numerical calculation provided a reasonable description to understand the cluster ionization (photoabsorption) and subsequent explosion dynamics [21,24]. An alternative x-ray light source using high-order harmonic generation (HHG) from an infrared laser was used to identify the explosion of clusters irradiated by short-wavelength laser pulses. Mass spectroscopy following the interaction of HHG light (at a wavelength of 38 nm and intensity of 0.1 TW/cm^2) with Xe clusters uncovered charge states up to Xe^{8+} [25], explained in terms of a lowering of the ionization potential (IP) in a strongly coupled cluster nanoplasma.

These results motivate a further investigation of photoionization in clusters subject to laser-driven plasma soft-x-ray laser pulses (at a wavelength of 13.9 nm, pulse width of ∼7 ps, and intensity of 10 GW/cm^2) and, in particular, how inner-shell ionization followed by Auger decay is affected by intense laser pulses. The photoionization cross section of 4*d* core electrons is ∼22 Mb at 90 eV, whereas for the outer electrons it is only ∼1.5 Mb [26]. Previous experiments have revealed that the production efficiency of Xe^{3+} ions arising from double Auger (DA) decay of 4*d* vacancies is significantly enhanced for large clusters [27]. In order to identify the mechanism underlying the enhancement and to attain a more comprehensive understanding of the x-ray laser and cluster interaction, electron energy spectroscopy is employed in the present study. It is found that for small clusters the spectral widths of 4*d* photoelectrons broaden with increasing cluster size. For large clusters greater than ∼10^4 atoms/cluster, no distinct line peak is observed, and the energy spectra follow a Maxwell-Boltzmann distribution. The plasma density calculated by a set of coupled rate equations and the resulting experimental electron temperature indicate that a strongly coupled cluster nanoplasma is generated. The lowering of the IP due to a plasma screening effect could be the cause of the drastic change in the Auger decay process.

II. EXPERIMENTAL SETUP

A laser-driven plasma soft-x-ray pulse having a wavelength of 13.9 nm ($h\nu$ = 89.2 eV), pulse width of ∼7 ps, and pulse energy of up to ∼300 nJ was generated by a transient collisional excitation scheme [28,29]. By using a chirped-pulse amplification laser with zigzag slab Nd:glass amplifiers, the maximum repetition rate of the x-ray laser was 0.1 Hz [30]. In order to improve the spatial coherence, an oscillator-amplifier configuration was employed, so that a highly coherent laser

beam with a small divergence of 0.2 mrad was obtained [31]. The highest laser intensity, focused using a Mo/Si multilayer spherical mirror, was 10 GW/cm^2 on target. A soft-x-ray charge-coupled device (CCD) camera measured the incoming laser energy and beam pattern.

Xenon clusters were generated by an adiabatic free expansion of high stagnation pressure gas at room temperature. A converging and diverging conical nozzle had a throat diameter of 0.2 mm and full-opening angle of 10°. The average cluster size was a function of the backing pressure at the nozzle and was estimated to range from $\langle N \rangle = 70$ up to 20 000 atoms/cluster [32,33]. To improve the spectral resolution, the cluster beam was collimated by two skimmers to extract the central part of the gas jet. It then interacted with the x-ray laser 25 cm downstream from the nozzle exit.

A time-of-flight (TOF) spectrometer was used to measure the electron spectra. The detector was a fast microchannel plate (MCP). The measurement was carried out in a direction parallel to the laser polarization axis. In order to suppress the collision of electrons with ambient gas during the cluster injection, the flight tube pressure was kept below 10^{-3} Pa by using a shroud vessel. TOF signals acquired in a single-shot mode were sorted according to laser intensity and averaged. Calibration of the flight time to determine the energy conversion was accomplished by measuring the photoelectron lines attributed to Xe 4*d* and 5*p* and He 1*s* electrons, in which the Xe and He effusive beams were irradiated by the laser pulses. Although the differential cross section for photoionization of atoms with linearly polarized radiation depends on the angle between the direction of polarization and the emitted electrons, the angular distribution parameter is nevertheless as small as 0.2 for photon energies of about 90 eV [34]. Figure 1 shows a schematic diagram of the experimental setup for the x-ray laser and cluster interaction.

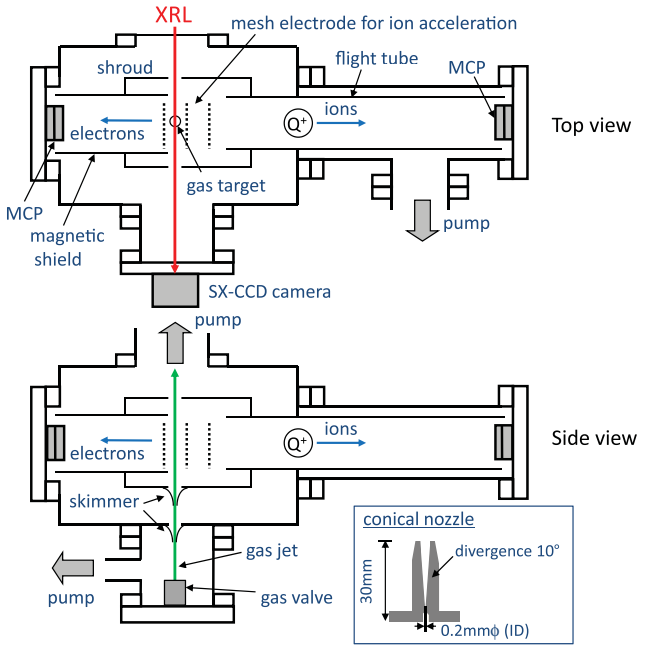

FIG. 1. (Color online) Schematic diagram of the experimental setup.

III. RESULTS AND DISCUSSION

Figure 2 shows the normalized TOF spectra obtained for various cluster sizes at a laser intensity of about 5 GW/cm^2. For comparison, the calculated energy curve is also plotted at the top, taking into account the photo lines attributed to Xe $4d^{-1}$ (at 19.65 eV for $^2D_{3/2}$ and at 21.64 eV for $^2D_{5/2}$), $5s^{-1}$ (65.8 eV), and $5p^{-1}$ (77.1 eV) and the energy resolution of the spectrometer. The relative intensities of representative $N_{45}OO$ Auger electrons are also shown [35], although they have not been scaled for direct comparison with the photoemission lines. The photoelectron peaks are clearly seen for small clusters, but no distinct Auger peaks are evident, due to the numerous decay channels from 4*d* vacancies into Xe^{2+} and Xe^{3+} states. With increasing cluster size, the profiles become broader than the expected linewidth: the experimental widths for $^2D_{5/2}$ at $\langle N \rangle = 20$ and 400 are 0.8 and 1.3 eV, respectively, while the instrumental width is estimated to be 0.72 eV. For the $\langle N \rangle = 1000$ cluster, the photolines of the spin-orbit 4*d* doublets merge significantly and tail toward the lower kinetic energies. Further increase of the cluster size results in the disappearance of the peaks and an increase in the strength of the low-energy component, indicating that cluster ionization is described by multiple electron emissions in a developing Coulomb field, whereby emitted electrons lose their kinetic energy [20]. The dependence of the energy spectra on the cluster size can be explained by a finite-size effect of the nanocluster. Compared with small clusters, the Coulomb field for larger ones is expected to be more effective because many ionization events occur in the larger volume.

In order to estimate the ionization events that occur during laser irradiation, a set of coupled rate equations involving a Xe atom, a Xe^{q+} ion, and an electron were solved. The cross sections of the collisional ionizations from the representative levels of the Xe^{q+} ion and atom were calculated using the empirical Lotz formula [36]. Photoionization of the Xe^+

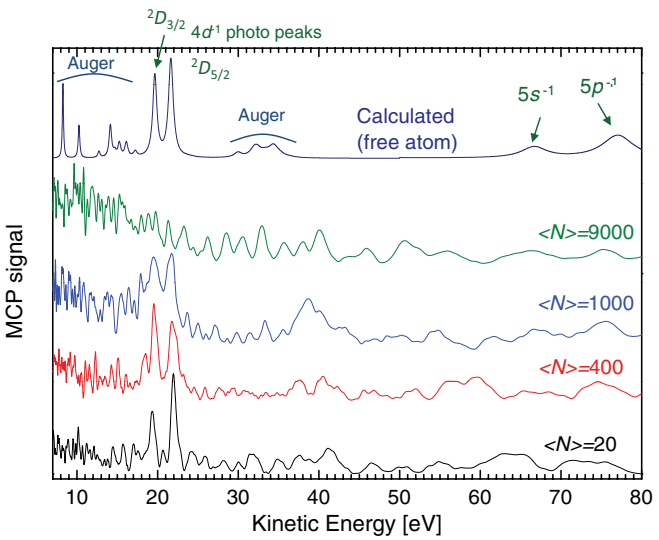

FIG. 2. (Color online) Electron TOF spectra observed for various cluster sizes at a laser intensity of 5 GW/cm^2. The MCP signals for the small clusters exhibit prominent photoemission peaks attributed to 4*d* electrons. With increasing cluster size, the photo linewidths of the 4*d* holes broaden beyond the instrumental limit.

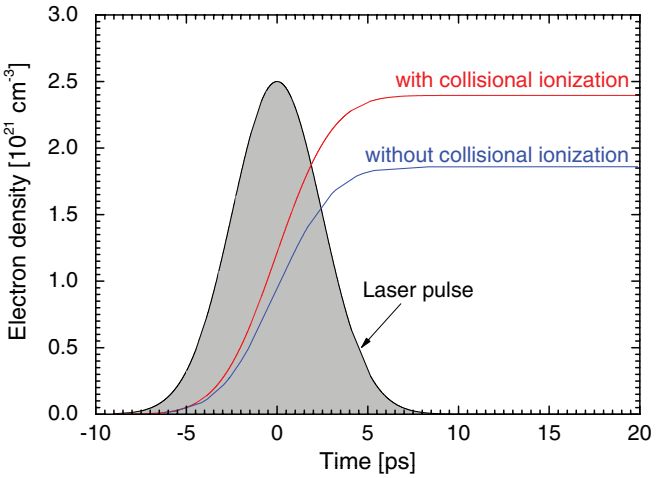

FIG. 3. (Color online) Time evolution of the electron density calculated from a set of coupled rate equations (with an initial atomic density of 1.7×10^{22} cm^{-3} and laser intensity of 10 GW/cm^2). Considering the collisional ionization due to electron impact, the density increased by 25% above that obtained by pure photoionization processes.

and Xe^{2+} ions was incorporated in the calculation. For a similar experiment using 13 nm FEL pulses, the degree of ionization reaches 97% for 50 PW/cm^2 (for a pulse width of 100 fs), so that the clusters rapidly disintegrate due to Coulomb repulsion or hydrodynamic expansion. For example, in the hydrodynamic case the expansion time is estimated to be around 8 ps for $Z_{ave} = 2.5$, $\langle N \rangle = 10^4$, and $T_e = 5$ eV [4]. However, the degree attainable in the present study is at most ~10% (for 10 GW/cm^2) and the rest of the cluster constituents remain neutral atoms. Thus the hydrodynamic expansion due to electron pressure is suppressed, since the surrounding atoms serve as a damper in the cluster. Consequently it is reasonable to neglect cluster expansion during the laser irradiation. On the other hand, by employing Xe-core–Ar-shell clusters, Hoener *et al.* found that charge-exchange recombination comes into play for core atoms in large clusters [37]. The most probable reaction is the following resonance one: $Xe^{2+} + Xe \rightarrow Xe^{+} + Xe^{+}$. The rate coefficient for this process is about 1×10^{-12} cm^3/s [38], yielding a charge-exchange time of only 60 ps, so that this process was not included. Figure 3 graphs the time evolution of the electron density for a laser intensity of 10 GW and a cluster atomic density of 1.7×10^{22} cm^{-3}. Many atoms within the cluster absorb the laser light due to the large photoionization cross section. The $4d$ inner-shell ionization results in the emission of two or three electrons by Auger decay. Therefore the electron density becomes as high as $n_e = 1.9 \times 10^{21}$ cm^{-3} after laser irradiation. Moreover, by taking collisional ionization into account, the density further increases by as much as ~25% ($n_e = 2.4 \times 10^{21}$ cm^{-3}). The number of photoions generated in 100-atom clusters at 10 GW/cm^2 is calculated to be ~5. Given that the kinetic energy of inner-ionized electrons is 20 eV and that the cluster has a uniform charge distribution (absent an expansion), quasifree electrons can outer ionize from the cluster surface. However, for 10^4 atoms/cluster, about 1000 electrons are generated, while only ~75 of them escape from the positively charged clusters, leading to the production of a plasma.

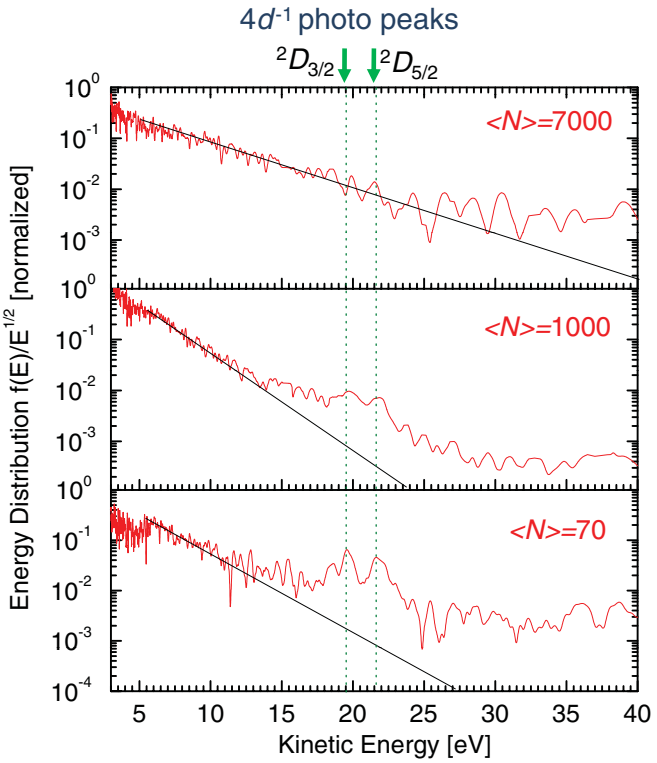

FIG. 4. (Color online) Electron energy distributions for cluster sizes of $\langle N \rangle = 70$, 1000, and 7000 at a laser intensity of 5 GW/cm^2. The vertical axis is a semilogarithmic plot of $f(E)/\sqrt{E}$. For large clusters, the photo peaks disappear and the distribution follows a Maxwell-Boltzmann profile.

The Maxwell-Boltzmann distribution $f(E)$ as a function of the energy E is

$$f(E) = \frac{2}{\sqrt{\pi}\,(k_B T_e)^{3/2}} \sqrt{E}\, \exp\left(-\frac{E}{k_B T_e}\right), \qquad (1)$$

where k_B is the Boltzmann constant and T_e is the electron temperature. Figure 4 is a semilogarithmic plot of $f(E)/\sqrt{E}$ for various cluster sizes at a laser intensity of 5 GW/cm^2. Prominent photopeaks at around 20 eV are observed for $\langle N \rangle = 70$ clusters. However, with increasing cluster size they become blurred and the energy distribution evolves into a Maxwellian straight line due to thermalization among electrons [21,39], indicating the formation of nanoplasmas. The deviation from the Maxwell distribution at high energies for small clusters is due to the decreased collision frequency of Coulomb interactions for fast electrons. Figure 5 shows the energy distribution for $\langle N \rangle = 2 \times 10^4$ clusters at laser intensities of 5 and 10 GW/cm^2. Best-fit lines for the respective laser intensities are also plotted in the figure. The higher the intensity, the higher the temperature was obtained: $k_B T_e = 6.5$ eV at 5 GW/cm^2 and 10 eV at 10 GW/cm^2. This trend in the laser intensity can be explained by further photoionization events in the clusters.

The coupling parameter between charged particles of species 1 and 2, Γ_{12}, describing the ratio of the interatomic potential energy to the thermal energy, is given by [40,41]

$$\Gamma_{12} = \frac{Z_1 Z_2 e^2}{4\pi\varepsilon_0 a k_B T_e}, \qquad (2)$$

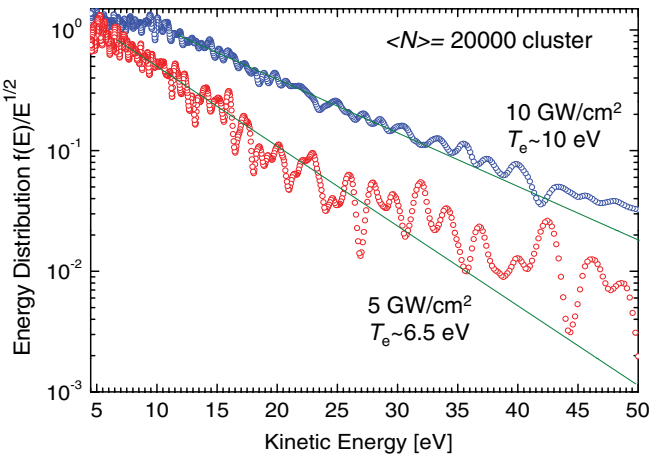

FIG. 5. (Color online) Energy distributions at laser intensities of 5 and 10 GW/cm^2 for a cluster having $\langle N\rangle$ 2 × 10^4. The straight lines correspond to electron temperatures of 6.5 and 10 eV.

where

$$a = \left(\frac{3\,(Z_1 Z_2)^{1/2}}{4\pi n_e}\right)^{1/3}. \qquad (3)$$

Here, Z is the electric charge, ε_0 is the permittivity of vacuum, and a is the ion sphere radius. The electron density after laser irradiation at an intensity of 10 GW/cm^2 reached 2.4 × 10^{21} cm^{-3}. Assuming the transient electron temperature to be 10 eV, a strongly coupled nanoplasma with Γ_{ee} = 0.31 and Γ_{ei} = 0.35 for Z = 2 should be generated due to photoabsorption of 4*d* electrons.

For such strongly coupled plasmas, the mass spectra show a peculiar distribution of ionic species: Xe^{3+} ions generated by double Auger decay of 4*d* vacancies are the dominant product for Xe clusters exposed to intense x-ray pulses [27]. The reduction of the ionization potential of outermost shell electrons due to the plasma screening effect [25,42–44] can account for this phenomenon. For example, the IP of Xe^{3+} ions in a Xe cluster plasma at a temperature of 30 eV is lowered from 32 to 8 eV [44], whereas the IP reduction for inner-shell electrons is less than a few eV because of the tight bonding with the atomic nucleus [45]. This reduction leads to an increase in the number of Xe^{3+} states accessible by the 4*d* holes, and thus (in a manner analogous to the decays of shake-up satellite states [46]) the DA transition probability for decays into Xe^{3+} states will increase. Consequently the mechanisms responsible for the enhancement of Xe^{3+} fragments in x-ray laser and cluster interactions may arise from the variation in the electronic energy structure of strongly coupled plasmas.

IV. SUMMARY

The interactions of Xe clusters with soft-x-ray laser pulses (13.9 nm, ∼7 ps, ⩽10 GW/cm^2) have been investigated, where the photoionization of inner 4*d* electrons dominates due to a giant resonance. In order to elucidate the ionization dynamics of clusters exposed to intense laser pulses, the electron energy spectra were measured. With increasing cluster size, the photoemission peaks attributed to 4*d* electrons broadens beyond the instrumental width. Above $\langle N\rangle = 10^4$, no prominent line emission is observed. These results suggest that the space charge created by the outer ionization of electrons from the clusters frustrates further electron emission. Indeed, numerical calculations based on rate equations show that a substantial fraction of the inner-ionized electrons cannot leave the cluster, resulting in the formation of a plasma. The temperature of these cluster nanoplasmas was T_e = 10 eV at 10 GW/cm^2 for $\langle N\rangle = 10^4$, implying that a strongly coupled cluster plasma with Γ_{ee} = 0.31 can be generated. Such extreme conditions, where the electronic energy structure is drastically distorted, may result in an anomalous enhancement of Xe^{3+} ion yields due to novel double Auger decay.

ACKNOWLEDGMENTS

This work was supported by a Grant-in-Aid for Scientific Research B (Grant No. 22340174) from the Japanese Society for the Promotion of Science. We would like to thank the JAEA x-ray laser research group for laser operations.

[1] D. Strickland and G. Mourou, Opt. Commun. **56**, 219 (1985).
[2] *Strong Field Laser Physics*, Springer Series in Optical Sciences Vol. 134, edited by T. Brabec (Springer, New York, 2008).
[3] U. Saalmann *et al.*, J. Phys. B **39**, R39 (2006).
[4] V. P. Krainov and M. B. Smirnov, Phys. Rep. **370**, 237 (2002).
[5] J. Purnell *et al.*, Chem. Phys. Lett. **229**, 333 (1994).
[6] B. D. McPherson *et al.*, Nature (London)**370**, 631 (1994).
[7] T. Ditmire *et al.*, Nature (London) **386**, 54 (1997).
[8] H. Wabnitz *et al.*, Nature (London) **420**, 482 (2002).
[9] T. Laarmann, A. R. B. de Castro, P. Gurtler, W. Laasch, J. Schulz, H. Wabnitz, and T. Moller, Phys. Rev. Lett. **92**, 143401 (2004).
[10] T. Laarmann, M. Rusek, H. Wabnitz, J. Schulz, A. R. B. de Castro, P. Gurtler, W. Laasch, and T. Moller, Phys. Rev. Lett. **95**, 063402 (2005).
[11] R. Santra and C. H. Greene, Phys. Rev. Lett. **91**, 233401 (2003).
[12] C. Siedschlag and J. M. Rost, Phys. Rev. Lett. **93**, 043402 (2004).
[13] D. Bauer, J. Phys. B **37**, 3085 (2004).
[14] M. Rusek and A. Orlowski, Phys. Rev. A **71**, 043202 (2005).
[15] C. Jungreuthmayer *et al.*, J. Phys. B **38**, 3029 (2005).
[16] B. Ziaja, H. Wabnitz, F. Wang, E. Weckert, and T. Moller, Phys. Rev. Lett. **102**, 205002 (2009).
[17] W. Ackermann *et al.*, Nat. Photonics **1**, 336 (2007).
[18] P. Emma *et al.*, Nat. Photonics **4**, 641 (2010).
[19] A. A. Sorokin, S. V. Bobashev, T. Feigl, K. Tiedtke, H. Wabnitz, and M. Richter, Phys. Rev. Lett. **99**, 213002 (2007).
[20] C. Bostedt *et al.*, Phys. Rev. Lett. **100**, 133401 (2008).
[21] C. Bostedt *et al.*, New J. Phys. **12**, 083004 (2010).
[22] H. Thomas *et al.*, J. Phys. B **42**, 134018 (2009).
[23] C. Bostedt *et al.*, J. Phys. B **43**, 194011 (2010).
[24] U. Saalmann J. Phys. B **43**, 194012 (2010).

[25] B. F. Murphy, K. Hoffmann, A. Belolipetski, J. Keto, and T. Ditmire, Phys. Rev. Lett. **101**, 203401 (2008).
[26] D. M. Holland *et al*., J. Phys. B **12**, 2465 (1979).
[27] S. Namba, N. Hasegawa, M. Nishikino, T. Kawachi, M. Kishimoto, K. Sukegawa, M. Tanaka, Y. Ochi, K. Takiyama, and K. Nagashima, Phys. Rev. Lett. **99**, 043004 (2007).
[28] T. Kawachi *et al*., Phys. Rev. A **66**, 033815 (2002).
[29] Y. Ochi *et al*., Appl. Phys. B **78**, 961 (2004).
[30] Y. Ochi *et al*., Appl. Opt. **46**, 1500 (2007).
[31] M. Nishikino, M. Tanaka, K. Nagashima, M. Kishimoto, M. Kado, T. Kawachi, K. Sukegawa, Y. Ochi, N. Hasegawa, and Y. Kato, Phys. Rev. A **68**, 061802(R) (2003).
[32] O. F. Hagena and W. Obert, J. Chem. Phys. **56**, 1739 (1972).
[33] F. Dorchies, F. Blasco, T. Caillaud, J. Stevefelt, C. Stenz, A. S. Boldarev, and V. A. Gasilov, Phys. Rev. A **68**, 023201 (2003).
[34] D. Rolles *et al*., Phys. Rev. A **75**, 031201(R) (2007).
[35] A. Kivimäki *et al*., J. Electron. Spectrosc. Relat. Phenom. **101-103**, 43 (1999).
[36] W. Lotz, Z. Phys. **206**, 205 (1967).
[37] M. Hoener *et al*., J. Phys. B **41**, 181001 (2008).
[38] D. Smith *et al*., J. Phys. B **13**, 2787 (1980).
[39] U. Saalmann *et al*., New J. Phys. **10**, 025014 (2008).
[40] S. Ichimaru and H. M. van Horn, *Strongly Coupled Plasma Physics* (University of Rochester Press, Rochester, NY, 1993).
[41] S. Ichimaru, Rev. Mod. Phys. **54**, 1017 (1982).
[42] A. V. Gets and V. P. Krainov, J. Phys. B **39**, 1787 (2006).
[43] I. Georgescu, U. Saalmann, and J. M. Rost, Phy. Rev. A **76**, 043203 (2007).
[44] P. Hilse *et al*., Laser Phys. **19**, 428 (2009).
[45] O. Björneholm *et al*., J. Chem. Phys. **104**, 1846 (1996).
[46] T. Luhmann, C. Gerth, M. Groen, M. Martins, B. Obst, M. Richter, and P. Zimmermann, Phys. Rev. A **57**, 282 (1998).